Rare Metal Materials and Engineering
Volume 51, Issue 1, January 2022
Available online at www.rmme.ac.cn

Science Press

Cite this article as: Zhang Jinlong, Qiu Risheng, Tan Xinu, et al. Microstructure Characterization of $Al_{0.3}$CoCrFeNi High-Entropy Alloy with Pulsed Laser Surface Treatment[J]. Rare Metal Materials and Engineering, 2022, 51(01): 30-35.

ARTICLE

Microstructure Characterization of $Al_{0.3}$CoCrFeNi High-Entropy Alloy with Pulsed Laser Surface Treatment

Zhang Jinlong[1,2], Qiu Risheng[1,2], Tan Xinu[1,2], Zhang Hui[1,2], Chai Linjiang[3], Bi Fengxian[1,2], Liu Qing[1,4]

[1] International Joint Laboratory for Light Alloys, Chongqing University, Chongqing 400044, China; [2] Electron Microscopy Center, Chongqing University, Chongqing 400044, China; [3] College of Materials Science and Engineering, Chongqing University of Technology, Chongqing 400045, China; [4] Key Laboratory for Light-Weight Materials, Nanjing Tech University, Nanjing 210009, China

Abstract: The as-cast $Al_{0.3}$CoCrFeNi high-entropy alloy (HEA) surface was treated by pulsed laser at four different powers (150, 250, 350, 450 W). According to the positions relative to the laser source, HEA structure could be transformed into three parts: the center of laser-affected zone with the cellular structure, the edge of laser-affected zone with the banded cellular structure along the grain boundary, and the unaffected area with original grains. Attributed to the rapid melting and solidification induced by pulsed laser, the cellular structure can be observed in all specimens processed at different powers. Additionally, the long cellular structures can be observed in the edge of the laser-affected zone. Then the specimens after pulsed laser surface treatment were annealed at 660 and 800 °C for 2 h, which leads to the precipitations along the boundaries of the cellular structure. The hardness test results show that the combined method of pulsed laser surface treatment with heat treatment improves the hardness of $Al_{0.3}$CoCrFeNi HEA remarkably.

Key words: high-entropy alloy; surface treatment; pulsed laser; microstructure; annealing

The high-entropy alloy (HEA) is an emerging metallic material composed of at least five principle elements with approximately equal molar ratio[1]. The primary properties including the high entropy, sluggish diffusion, lattice distortion, and cocktail effects of HEA ensure that the alloy has remarkable mechanical strength, excellent corrosion resistance, and good creep properties[2-6]. Compared with the conventional structure alloys and other HEAs, $Al_{0.3}$CoCrFeNi HEA with face-centered cubic structure has high strength, high ductility, and good corrosion resistance due to its unique chemical composition and structure[7] and thereby attracts a lot of attention in improving the alloy properties by controlling microstructure through different processes, including plastic deformation and heat-treatment. For instance, Li et al[8] produced $Al_{0.3}$CoCrFeNi HEA fibers by hot-drawing for cryogenic applications with the strength and ductility of 1600 MPa and 17.5%, respectively. The great improvement is due to the change in deformation mechanism from the planar slip of dislocations to nano-twinning. Tang et al[9] improved the hardness of $Al_{0.3}$CoCrFeNi HEA to 6000 MPa, which is approximately four times larger than that of the as-cast alloy. This enrichment is beneficial from the nanostructure produced by high-pressure torsion and thermal annealing. During the past decades, researches achieved great success in improving HEA properties by different processing methods. However, the application of the surface treatment, especially the pulsed laser surface treatment which can effectively modify the properties of the alloy surface, for $Al_{0.3}$CoCrFeNi HEA is still restricted.

The pulsed laser surface treatment is recognized as an efficient and convenient method for surface modification in various fields[10-13]. The Zr702 alloy has three different microstructure zones of fine α plates, irregular-shaped grains, and unchanged equiaxed grains. These mentioned zones were investigated from the surface to the substrate after pulsed laser surface treatment to improve the hardness of Zr702 alloy from

Received date: January 09, 2021
Foundation item: National Natural Science Foundation of China (51421001); 111 Project Sponsored by Ministry of Education and State Administration of Foreign Experts Affairs of China (B16007)
Corresponding author: Qiu Risheng, Ph. D., Professor, International Joint Laboratory for Light Alloys, Chongqing University, Chongqing 400044, P. R. China, E-mail: rsqiu@cqu.edu.cn

1500 MPa to 3500 MPa[14]. In addition, the refined austenite and martensite can be observed in the surface of the 40CrNiMo7 steel after pulsed laser surface treatment which achieves a remarkable advancement in hardness from 3000 MPa to 10 000 MPa[15]. The planar crystals, columnar dendrites, and equiaxed crystals can be observed in the FeCoNiCrMn HEA coatings prepared by high speed laser cladding which also improves the properties of HEA coatings[16]. Pulsed laser surface treatment is an efficient method to modify the surface properties through the grain refinement and dislocation movement[17-19].

The microstructure evolution of the $Al_{0.3}CoCrFeNi$ HEA after pulsed laser surface treatment was investigated for improving the properties of as-cast $Al_{0.3}CoCrFeNi$ HEA in this research. The morphologies of $Al_{0.3}CoCrFeNi$ HEA after pulsed laser surface treatment at different powers were observed. After pulsed laser surface treatment, the $Al_{0.3}CoCrFeNi$ HEA specimens were annealed at 660 and 800 °C for 2 h to investigate the function of heat treatment to the microstructure of alloys. The hardness of different regions of $Al_{0.3}CoCrFeNi$ HEA specimens was measured to analyze the relationship between mechanical properties and microstructure modified by combined method of pulsed laser surface treatment with annealing treatment.

1 Experiment

The as-cast $Al_{0.3}CoCrFeNi$ HEA consisted of pure elements (99.9wt%). The rectangular specimens with a dimension of 10 mm×10 mm×20 mm were cut from the as-cast alloy. Before pulsed laser surface treatment, the specimens were polished carefully to eliminate the impurities. The specimen surface with a dimension of 10 mm×20 mm was irradiated by a pulsed laser device (600 W Nd: YAG) at four different powers (150, 250, 350, 450 W). The beam diameter was 2 mm, the beam travel speed was 8 mm/s, the pulse frequency was 20 Hz, and the power density was 191.1, 318.5, 445.9, 573.3 W/mm^2 at laser power of 150, 250, 350, and 450 W, respectively. After the pulsed laser surface treatment, the specimens were annealed at 660 and 800 °C for 2 h and then quenched in air.

The microstructures of specimens processed by pulsed laser and annealing treatments were characterized by TESCAN Mira 3 scanning electron microscope (SEM) coupled with electron backscattered diffraction (EBSD) detector. After mechanical polish by SiC paper of 3000# for the final step, the specimens for SEM observation were electropolished. The hardness of the specimens was tested by the MH-5L Vickers indentation tester with a load of 500 g for 10 s. In order to compare the hardness of the original grains and laser-affected structures, more than 20 indentations with an interval of 500 μm from each other were produced on the surface of each specimen.

2 Results and Discussion

2.1 Microstructure characterization

Fig. 1 exhibits the cross-sectional microstructure of specimens after pulsed laser surface treatment at different powers. Apparently, the as-cast $Al_{0.3}CoCrFeNi$ HEA consists of coarse grains with the diameter from 400 μm to 2000 μm. The morphologies and sizes of the laser-affected zone (LAZ), surrounded by the dashed line, can be observed in Fig. 1. The LAZs of specimens treated at different powers have similar cone-like morphologies. It can be observed that the maximum LAZ width of specimens treated at 150, 250, 350, and 450 W is about 400, 600, 800, and 1000 μm, respectively; the maximum LAZ depth of specimens treated at 150, 250, 350, and 450 W is about 500, 800, 1100, and 1600 μm, respectively. The range of LAZ area on the surface is increased with increasing the power of pulsed laser. Attributed to the large energy density of pulsed laser at high power, the specimen treated at 450 W possesses the largest LAZ area.

As shown in Fig. 2, the cellular structures with distinctions can be observed in all specimens after pulsed laser surface treatment by SEM at backscattered electron (BSE) mode. The average diameters of the cellular structure of specimens treated at 150, 250, 350, and 450 W are about 1.2, 1.5, 2.5, and 3.2 μm, respectively. The results illustrate that the formation of the cellular structure is related to the power density of the pulsed laser. The higher the laser power, the larger the size of the cellular structure. In brief, the formation of the cellular structure in the $Al_{0.3}CoCrFeNi$ HEA after pulsed laser surface treatment is determined by the energy density of pulsed laser. In other researches, the cellular structure with 0.5

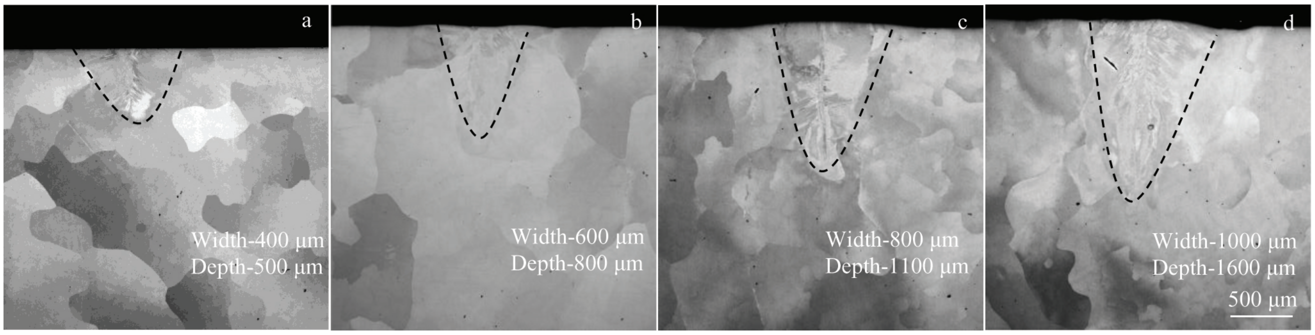

Fig.1 SEM microstructures of the cross-section of the specimens after pulsed laser surface treatment at different powers: (a) 150 W, (b) 250 W, (c) 350 W, and(d) 450 W

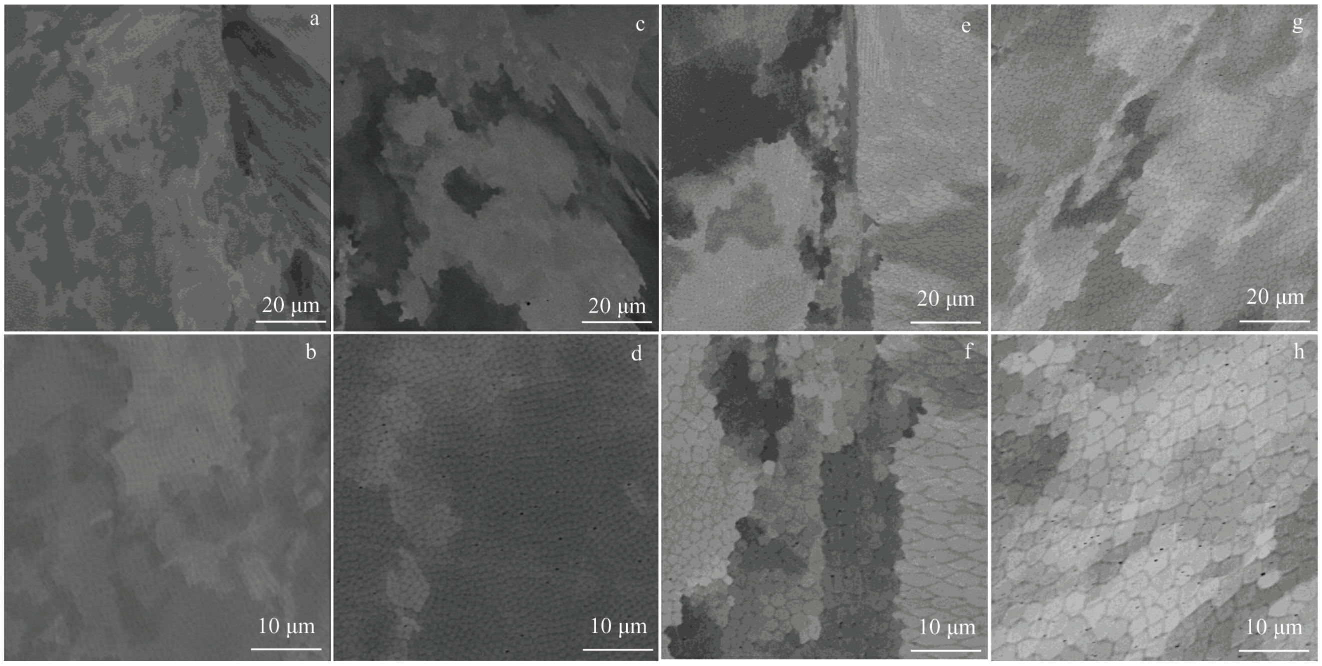

Fig.2 SEM microstructures of specimens after pulsed laser surface treatment at different powers: (a, b) 150 W, (c, d) 250 W, (e, f) 350 W, and (g, h) 450 W

μm in diameter can be detected in austenitic 316L stainless steel after laser powder bed fusion treatment which achieves an optimal improvement of strength and ductility through element segregation and dislocations among the boundaries of cellular structure[20-23]. In addition, the cellular structure can also be observed in CrCoNi medium-entropy alloy treated by pulsed laser surface treatment at 200 and 400 W, which is probably generated by rapid melting and solidification during the surface modification procedure[24].

Fig. 3 shows SEM morphologies of cellular structure of different specimens. As shown in Fig.3a and 3b, the region of the long cellular structure is indicated to show the relative position of normal cellular structure and the long cellular structure. Fig. 3c shows the long cellular structure which is different from the conventional cell-like structure and discovered in the LAZ of specimens. In Fig. 3d, the long cellular structure and conventional cellular structure lie on different edges of the grain boundary. Furthermore, it is found that the long cellular structure is usually detected in the edge of LAZ close to the grain boundary, which results in the formation of long cellular structure through the heat conduction during the surface treatment. The formation of cellular structure inside the grain can provide an excellent combination of strength and ductility due to the rapid melting and solidification[23-26]. The cellular structure in alloys is mostly net-like, but the long cellular structure in $Al_{0.3}CoCrFeNi$ HEA is barely reported. Furthermore, the formation of long cellular structure in the edge of LAZ of specimens is due to the effect of heat conduction. The formation of the cellular structure is affected by the rapid melting and solidification during the surface treatment. In the center of LAZ with high energy density, the heat is diffused homogeneously, leading to the formation of intensive cellular structure. In addition, in the edge of LAZ, the heat conduction is weakened, resulting in the temperature gradient at solid-liquid interface which provides the advantageous condition for the growth of long cellular structure. In consequence, the long cellular structures are generated by the condensate depression

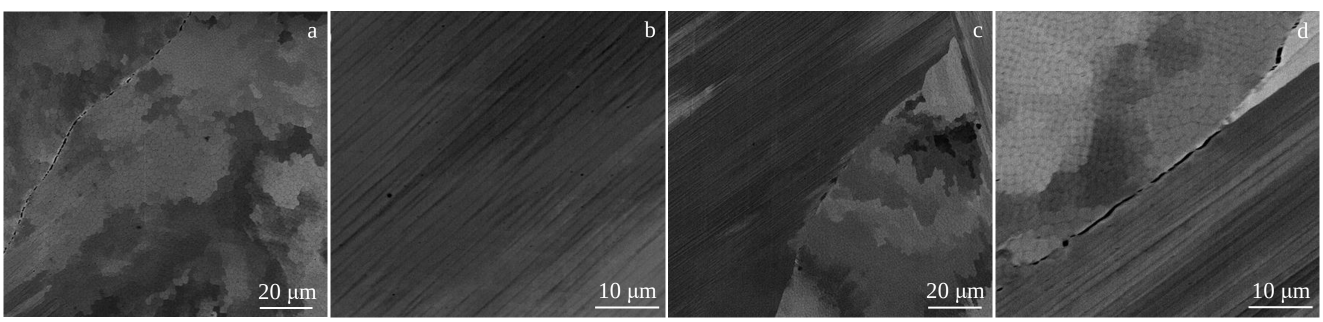

Fig.3 SEM morphologies of cellular structure of specimens after pulsed laser surface treatment at 250 W (a, b) and 350 W (c, d)

caused by the gradually weakened heat conduction because of the progressively lengthened distance from the laser source to the region close to the LAZ edge.

EBSD maps of the orientation-related microstructure features of the specimen treated by pulsed laser at 150 W are shown in Fig. 4. In Fig. 4a, the microstructure of the cellular structure can be observed in LAZ of $Al_{0.3}CoCrFeNi$ HEA after pulsed laser surface treatment. According to the inverse pole figure (IPF) of Fig. 4b, the cellular structures inside the large grains can barely be distinguished and the cellular structures beside the grain boundary show different orientations which are consistent with those of the original grains. As shown in Fig.4c, the misorientation of the cellular structures close to the grain boundary is greater than that in the center of the original grains. Besides, the power density of laser treatment is closely related to the mighty misorientation among the cellular structures. Generally, the pulsed laser surface treatment is an efficient method to promote the performance through the microstructure changes of materials. For conventional large grains, the grain refinement is the primary method for the improvement of strength and hardness. The pulsed laser surface treatment provides a novel method for strengthening the properties of $Al_{0.3}CoCrFeNi$ HEA through cellular structure and substructure precipitated intensively in the large grains. However, the grain size of the as-cast $Al_{0.3}CoCrFeNi$ HEA ranges from 500 μm to 2000 μm, which is larger than that of LAZ. In consequence, the cellular structures inside the original grains induced by pulsed laser at different powers can change the properties of as-cast $Al_{0.3}CoCrFeNi$ HEA.

Fig. 5 exhibits SEM images of $Al_{0.3}CoCrFeNi$ HEA specimens after pulsed laser surface treatment at 350 and 450 W followed by annealing at 660 °C for 2 h. The conventional cellular structures and long cellular structures divided by the grain boundary can still be observed in the specimens after annealing treatment. In addition, the precipitations can be observed along the grain boundary in both specimens after heat treatment. The hysteresis diffusion effect of HEAs results in the subtle changes of microstructures of HEA after pulsed laser surface treatment and heat treatment.

SEM images of specimens after pulsed laser surface treatment at 350 and 450 W followed by annealing at 800 °C for 2 h are shown in Fig.6. The precipitations can be observed in the edge of the cellular structures. The boundaries of the cellular structures disappear during the heat treatment and the emerging precipitations formed by the element diffusion and segregation in both conventional cellular structure and long cellular structure occur. Notably, the distribution of the precipitations is primarily determined by the cellular structures produced by the pulsed laser surface treatment. In the long cellular structure, the precipitations along the boundaries promote the formation of layer structures consisting of substrate and precipitations, which affects the morphologies and properties of HEA. The distance between the adjacent precipitations is determined by the energy density of the laser power which greatly affects the size of the cellular structures. In addition, the distinctions between the cellular structures gradually disappear during the heat treatment with the vanishment of boundaries. In consequence, the subsequent heat treatment can change the cellular structures produced by pulsed laser, which facilitates the formation of the precipitations and improves the properties of as-cast $Al_{0.3}CoCrFeNi$ HEA with coarse grains.

2.2 Hardness analysis

The schematic diagram of hardness indentation sites of specimens is shown in Fig. 7a for the hardness test. The hardness variation curves of the specimens treated by pulsed laser at 150, 250, 350, and 450 W are displayed in Fig.7b, and those of the specimens treated by pulsed laser at 350 and 450 W and subsequent annealing at 660 and 800 °C for 2 h are exhibited in Fig. 7c. It is obvious that the hardness of the center of LAZs is higher than that of the substrate on both sides of all specimens. The maximum hardness of specimens treated by pulsed laser at 350 and 450 W reaches 1587 and 1584 MPa, respectively; while the hardness of the substrate treated by pulsed laser at 350 and 450 W is 1325 and 1258 MPa, respectively. This phenomenon is ascribed to the formation of the dense cellular structures inside the coarse grains. The original grain size is unchanged during the pulsed laser surface treatment because the size of the coarse grains is larger than that of LAZ. Therefore, the cellular structure can improve the hardness of the as-cast $Al_{0.3}CoCrFeNi$ HEA without changing the grain size, which greatly influences the

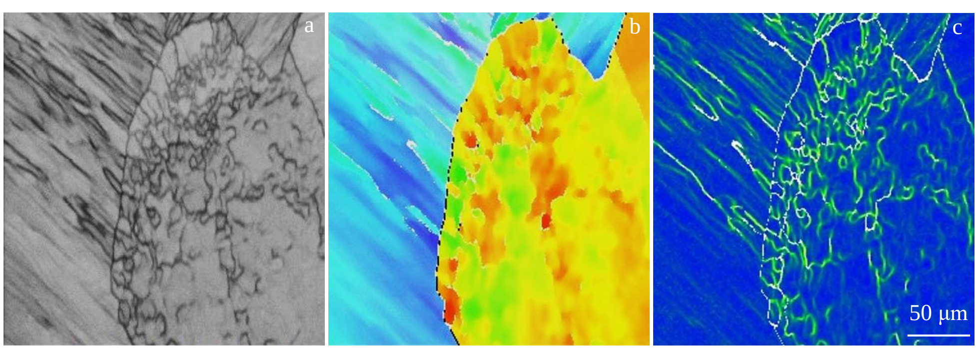

Fig.4 EBSD images of specimen after pulsed laser surface treatment at 150 W: (a) band contrast, (b) IPF, and (c) local misorientation

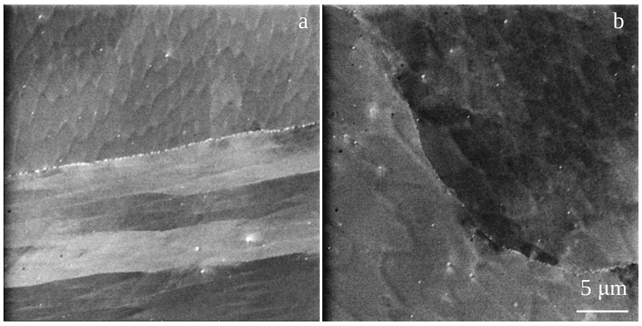

Fig.5 SEM images of specimens after pulsed laser surface treatment at 350 W (a) and 450 W (b) followed by annealing at 660 °C for 2 h

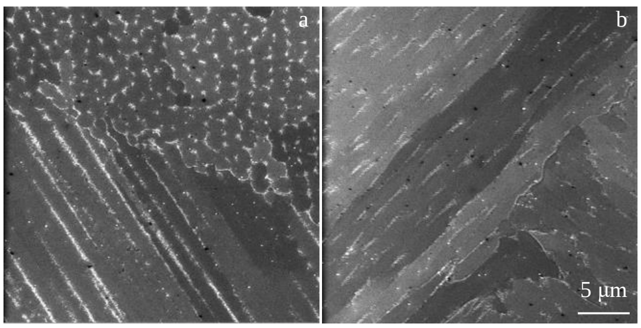

Fig.6 SEM images of specimens after pulsed laser surface treatment at 350 W (a) and 450 W (b) followed by annealing at 800 °C for 2 h

original performance of $Al_{0.3}CoCrFeNi$ HEA. In addition, the hardness of the substrate is primarily determined by the orientation of the original grains beside LAZ. The hardness of LAZ depends on the cellular structures with similar size and orientation, which indicates that the cellular substructure produced by pulsed laser can improve the mechanical properties of $Al_{0.3}CoCrFeNi$ HEA with coarse grains. In general, the traditional approaches can optimize the mechanical properties through modification of grain sizes, dislocation distribution, and recrystallization. The pulsed laser surface treatment can adjust the substructure inside the original grains, providing a novel strategy for strengthening alloys more precisely. Bertsch et al[23] reported that the 316L stainless steels fabricated by the laser powder-bed-fusion technique exhibit a remarkable combination performance of yield strength and tensile ductility, which is primarily attributed to the nanoscale cellular structures with 150 nm in diameter. The great improvement is ascribed to the high density energy provided by laser treatment and to the precipitation segregation of enrichment of O and Si elements around the boundary of cellular structure with aggregation of Cr and Mo elements.

Fig. 7c shows the hardness of specimens after pulsed laser surface treatment and annealing treatment. The hardness of LAZ is obviously higher than that of the substrate of specimens after annealing, which is attributed to the cellular structures. In addition, the maximum hardness of the specimens annealed at 660 and 800 °C reaches 1988 and 1743 MPa, respectively. The hardness of substrate and LAZ is improved and the hardness improvement of LAZ is more sensitive to the degree of heat treatment and the cellular structures. During the heat treatment process, the dislocation is gathered and becomes weakened in the cellular structures, resulting in the decrease in specimen hardness. The cellular structures produced by pulsed laser is decreased during the annealing procedure, while the precipitation generated in the boundaries of the cellular structures replaces the cellular structure. Thus, the hardness is improved. The hardness improvement of the specimens annealed at 660 and 800 °C is determined by the cellular structure and precipitations. During the annealing treatment, the cellular structure is weakened and the precipitation is increased. More cellular structures exist in the specimen annealed at 660 °C than in the specimen annealed at 800 °C. Therefore, the hardness improvement of specimen annealed at 660 °C is greater than that at 800 °C. In contrast, the precipitation in specimen annealed at 800 °C is more intensive than that at 660 °C, which decreases the hardness of specimen annealed at 800 °C. As a result, the hardness of specimens annealed at 660 °C is higher than that

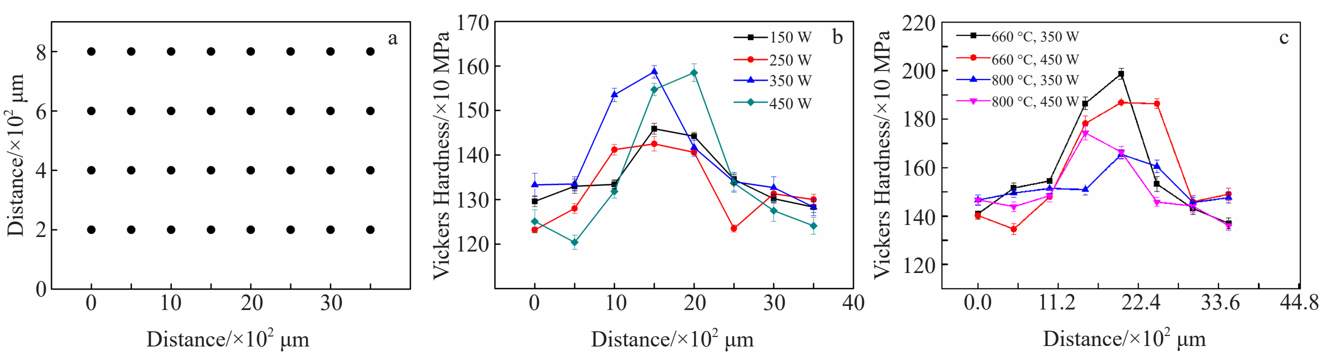

Fig.7 Schematic diagram of indentation sites for hardness tests (a) and surface hardness of substrate and LAZs in specimens after different treatments: (b) pulsed laser surface treatment at different powers; (c) pulsed laser surface treatment at 350 and 450 W followed by annealing at 660 and 800 °C for 2 h

of the specimen annealed at 800 °C. The mutual effect of the weakened cellular structure and less precipitation formation in specimen can promote the properties of $Al_{0.3}CoCrFeNi$ HEA with coarse grains.

3 Conclusions

1) The cellular structures of $Al_{0.3}CoCrFeNi$ high-entropy alloy can be observed after pulsed laser surface treatment at different laser powers. In the specimens treated by pulsed laser at 250 and 350 W, the long cellular structures close to the grain boundary are produced by the effect of heat conduction during the surface treatment and can be detected on the edge of laser-affected zone .

2) The precipitation segregation can be observed in the boundaries of the cellular structures of specimens after annealing treatment at 660 and 800 °C for 2 h, which replaces the cellular structure and results in the hardness improvement.

References

1 Annasamy M, Haghdadi N, Taylor A *et al*. *Materials Science and Engineering A*[J], 2019, 745: 90

2 Gangireddy S, Gwalani B, Liu K *et al*. *Materials Science and Engineering A*[J], 2018, 734: 42

3 Yasuda H Y, Shigeno K, Nagase T. *Scripta Materialia*[J], 2015, 105: 80

4 Shun T T, Hung C H, Lee C F. *Journal of Alloys & Compounds*[J], 2010, 495(1): 55

5 Xu X X, Mu X Q, Zhu C. *Rare Metal Materials and Engineering*[J], 2020, 49(12): 4005

6 Zhao Bin, Zhu Dezhi. *Rare Metal Materials and Engineering*[J], 2019, 48(12): 4004 (in Chinese)

7 Gwalani B, Soni V, Lee M *et al*. *Materials and Design*[J], 2017, 121: 254

8 Li D Y, Li C X, Feng T *et al*. *Acta Materialia*[J], 2017, 123: 285

9 Tang Q H, Huang Y, Huang Y Y *et al*. *Materials Letters*[J], 2015, 151: 126

10 Yao Y, Li X, Wang Y Y *et al*. *Journal of Alloys & Compounds*[J], 2014, 583: 43

11 Lee S J, Park C J, Lim Y S *et al*. *Journal of Nuclear Materials*[J], 2003, 321(2-3): 177

12 Khairallah S A, Anderson A T, Rubenchik A *et al*. *Acta Materialia*[J], 2016, 108: 36

13 Liu W J, Zong X W, Yang Y M *et al*. *Rare Metal Materials and Engineering*[J], 2020, 49(12): 4031

14 Chai L J, Chen B F, Wang S Y *et al*. *Applied Surface Science*[J], 2016, 364: 61

15 Wang H H, Hao S Z. *Nuclear Instruments and Methods in Physics Research Section B*[J], 2017, 403: 45

16 Cui Z Q, Qin Z, Dong P *et al*. *Materials Letters*[J], 2020, 259: 126 769

17 Lyu P, Chen Y N, Liu Z J *et al*. *Applied Surface Science*[J], 2020, 504: 144 453

18 Cropper M D. *Applied Surface Science*[J], 2018, 455: 153

19 Ni C, Shi Y, Liu J *et al*. *Optics and Laser Technology*[J], 2018, 105: 257

20 Ma L L, Gao Z J, Hu S H *et al*. *Materials Research Express*[J], 2019, 5(6): 56 540

21 Yasuda H Y, Miyamoto H, Cho K *et al*. *Materials Letters*[J], 2017, 199: 120

22 Annasamy M, Haghdadi N, Taylor A *et al*. *Materials Science & Engineering A*[J], 2019, 745: 90

23 Bertsch K M, de Bellefon G M, Kuehl B *et al*. *Acta Materialia*[J], 2020, 199: 19

24 Wang Y M, Voisin T, McKeown J T *et al*. *Nature Materials*[J], 2018, 17(1): 63

25 Chai L J, Xiang K, Xia J Y *et al*. *Philosophical Magazine*[J], 2019, 99(24): 3015

26 Wang H H, Hao S Z. *Nuclear Instruments and Methods in Physics Research Section B*[J], 2017, 403: 45

激光表面处理$Al_{0.3}CoCrFeNi$高熵合金组织特征

张金龙[1,2]，邱日盛[1,2]，谭希努[1,2]，张　惠[1,2]，柴林江[3]，毕凤仙[1,2]，刘　庆[1,4]

(1. 重庆大学 轻合金材料国际合作联合实验室，重庆 400044)

(2. 重庆大学 电子显微镜中心，重庆 400044)

(3. 重庆理工大学 材料科学与工程学院，重庆 400045)

(4. 南京工业大学 先进轻质高性能材料研究中心，江苏 南京 210009)

摘　要：通过4种不同功率的脉冲激光（150，250，350，450 W）对铸态$Al_{0.3}CoCrFeNi$高熵合金进行处理。按相对于激光源的位置，合金组织分为3个部分：内部具有细胞状结构的中心影响区，具有长条结构的边缘影响区，以及未受影响的原始晶粒区域。由于激光引起的快速熔化和凝固，经不同功率处理的样品截面中均观察到细胞结构；另外，在激光影响区边缘发现了长条细胞结构。之后，将激光处理的样品分别在660和800 ℃下退火2 h，可以观察到沿细胞结构边界有沉淀相析出。通过硬度测试，表明激光表面处理和后续热处理相结合的方法显著提升了合金的硬度。

关键词：高熵合金；表面处理；脉冲激光；微观结构；热处理

作者简介：张金龙，男，1995年生，硕士，重庆大学电子显微镜中心，重庆 400044，E-mail：20152739@cqu.edu.cn